ISSN:2231-0711

Yaser E. Al-Shaikh et al | IJCSET(www.ijcset.net) | November 2016 | Vol 6, Issue 11, 380-386

Design of a Metamaterial Enhanced Triple Band Printed MIMO Antenna for WiFi and WiMAX Applications

Yaser E. Al-Shaikh[#1], Lubab A. Salman[*2]

[#]*Department of Electronic and Communications Engineering, College of Engineering, Al-Nahrain University, Baghdad-Iraq*

[*]*Department of Electronic and Communications Engineering, College of Engineering, Al-Nahrain University, Baghdad-Iraq*

***Abstract*—The development of a miniaturized two-element printed MIMO antenna with a triple-band performance for WiFi and WiMAX operability is presented in this paper. The proposed antenna configuration incorporates two small-sized square copper patches printed on a standard FR-4 substrate with an overall size of 40×27.2 mm^2. The two patches are furnished with slots into the form of split-ring resonators and fed from two extended microstrip lines with trimmed ground planes to allow for triple-band operation. A neutralizing line connecting the two patches is also incorporated into the antenna structure to improve isolation. Double-sided metamaterial grid is included to fill the space between the two antenna elements providing thereby for enhanced radiation efficiency and improved isolation for the second band. Practical results clearly depict the triple band performance with a slight slip in the second and third bands form the ones predicted by simulation covering the following ranges of frequencies: (2.4-2.485) GHz, (5.1-5.35) GHz for Wi-Fi (IEEE 802.11) and (3.35-3.8) GHz for Wi-max (IEEE 802.16.2005).**

***Keywords*— Printed Antenna, Metamaterial, Neutralizing Line, Split Ring Resonator, MIMO, WiFi, WiMAX**

I. INTRODUCTION

The performance of wireless communication systems could to a far extent be improved by the employment of multiple-input multiple-output (MIMO) technology. MIMO antennas play a central role in enabling this technology representing the RF frontend of MIMO transceivers implemented by an increasing number of wireless devices such as WiFi and WiMAX routers. The commercially available designs, however, employ monopole antennas with wide enough separation to increase isolation and improve diversity, what makes them quite bulky for surface mounted or very slim installations. A printed miniaturized MIMO antenna with good inter-element isolation would help to reduce the footprint of such devices making them more amenable for non-protruding installations.

Closely spaced antennas, however, will cause unwanted mutual coupling and low antenna efficiency, thus reducing the performance of the MIMO system. To reduce the mutual coupling, various methods had been proposed in the literature. Capacitive loaded loops used on the top side and in the ground plane of the printed antenna to improve the isolation of the two bands were proposed in [1]. Hybrid fractal shape planar monopole antenna where T-shape strip is inserted and rectangular slot is etched at top side of ground plane to respectively to improve the impedance matching and isolation between the antennas were proposed in [2]. In [3], defected ground structure was used to suppress the effect of the surface current between elements of the proposed antenna. Also [4-7] presented four-element MIMO antenna configurations which incorporated neutralization line, meander line resonator, and a decoupling network as isolators. The development of metamaterial enhanced MIMO antennas has been a viable area of research over the past decade, too. Antenna engineers and researchers had come up with a variety of designs employing a variety of techniques to meet the needs of different design applications. The metamaterial was employed in those designs to reduce the mutual coupling, to minimize the antenna size, and to enhance the antenna bandwidth and efficiency as in [8-10], where rectangular loop, spiral and s-shaped resonators placed in the space between the antenna elements to provide high levels of isolation. Metamaterial was also inspired as part of the patch surface of small printed monopole antennas as in [11]. In [12] split ring resonators were used to improve the MIMO antenna efficiency and to reduce the mutual coupling between its elements.

This work presents a new attempt to achieve even more miniaturization, greater inter-element isolation, and improved radiation efficiency through the utilization of a metamaterial configuration in the design of a triple-band two-element printed MIMO antenna. The metamaterial design will be sought to be part of one or both of the antenna printed layers (on either side of a standard substrate material). In contrast to some of the designs proposed in the published literature which incorporate vertically aligned metamaterial slabs to form the substrate which is both costly and high-profile, the design to be investigated in this work should prove much less complicated and low-profile, a feature widely sought by many communication systems applications. The frequency bands that are intended to be covered by this design include two WiFi bands and two WiMAX band, namely, the bands depicted in Table1.

Table 1 WiFi and WiMAX Standard Operating Bands [13] [14].

System	Design Operating Bands	Frequency Range (GHz)	
WiFi IEEE 802.11	2.4 GHz	2.4-2.485	
	5 GHz	5.2 GHz	5.15-5.35
		5.5 GHz	5.47-5.725
		5.8 GHz	5.725-5.875
WiMAX IEEE 802.16	3.5 GHz	3.4-3.6	
	3.7 GHZ	3.6-3.8	

II. The Triple-Band Antenna Characteristics

The triple-band printed MIMO antenna design is started with the development of a single-element microstrip antenna with a rectangular patch of width W=36.6 mm and length L=27.6mm, printed on a dielectric substrate of thickness h=1.6 mm^2 and relative permittivity ε_r=4.4, to operate with a resonance frequency of 2.45 GHz. For the MIMO design two such elements are used, and for the triple band performance split-ring resonators (SRRs) are introduced into the patch area. A neutralizing line and a metamaterial mat are also incorporated into the final antenna design to improve the 10 dB impedance bandwidth, gain, and efficiency and to minimize the antenna size. The triple-band performance of the antenna will be thoroughly investigated to identify the parameters affecting the introduction of each band in the frequency response of the proposed antenna. This step is then followed by a fine tuning step to achieve the required triple band operation.

A. The Two-Element MIMO Antenna without SRR

The initial MIMO antenna configuration in this case is depicted in Fig. 1 and its dimensions are given in Table 2. The simulated reflection coefficient performance of the antenna patch without SRR is shown in Fig. 2 where it can be seen that there is a single band covering the range 2.22-2.78 GHz and amounting to a total bandwidth of 560 MHz.

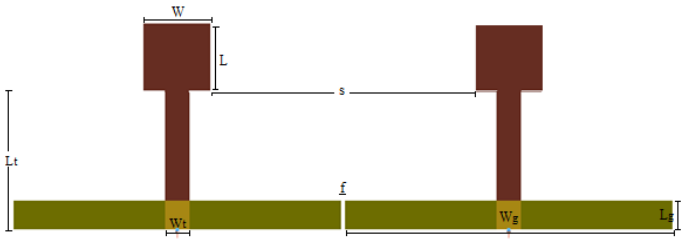

Figure 1 The configuration of two-element MIMO antenna without the SRR.

Table 2 The parameter setting of the MIMO antenna of Fig. 1.

Parameter	Value (mm)
W	9
L	9
f	0.5
s	31.5
W_t	2.95
L_t	16.7
W_g	40
L_g	3.5

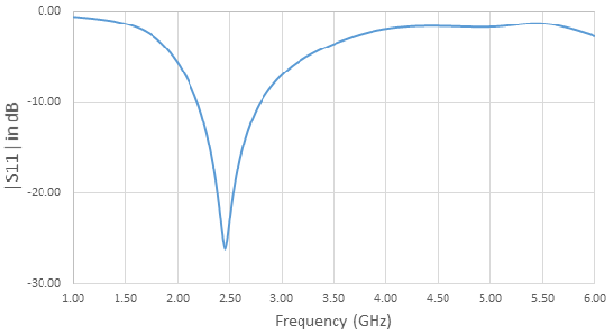

Figure 2 The reflection coefficient responses of the two-element MIMO antenna without the SRR.

B. The Two-Element MIMO Antenna with Single Internal SRR

The MIMO antenna configuration in this case is depicted in Fig. 3 and its dimensions are given in Table 3. The simulated reflection coefficient performance of the antenna with single internal SRR is shown in Fig. 4 for different values of the SRR width parameter, *a*. Evidently, there is a single usable band between 2 and 3 GHz, and only a notch in the response starts to appear between 4 and 5 GHz moving upward with the increment of *a*. This notch will not turn into a fully usable band until the addition of the second (external) SRR.

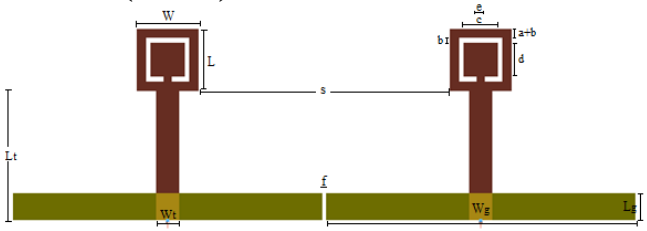

Figure 3 The configuration of two-element MIMO antenna with single internal SRR.

Table 3 The parameter setting of the MIMO antenna of Fig. 3.

Parameter	Value (mm)	Parameter	Value (mm)
W	9	W_g	40
L	9	L_g	3.5
e	1	a	0.3
f	0.5	b	0.6
s	31.5	c	5.4
W_t	2.95	d	5.4
L_t	16.7		

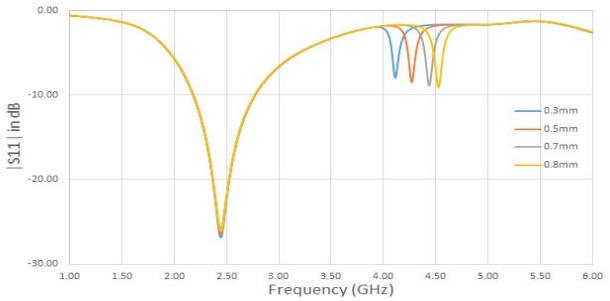

Figure 4 The reflection coefficient responses of the two-element MIMO antenna with single internal SRR for different SRR widths (*a*).

C. The Two-Element MIMO Antenna with Single External SRR

The MIMO antenna configuration in this case is depicted in Fig. 5 and its dimensions are given in Table 4. The simulated reflection coefficient performance of the antenna patch with single external SRR is shown in Fig. 6 for different values of the SRR width parameter, *a*. Evidently, there are two usable bands, one between 2 and 2.5 GHz while the other one is between 3 and 4 GHz. The second band is moving upward with the increase in a.

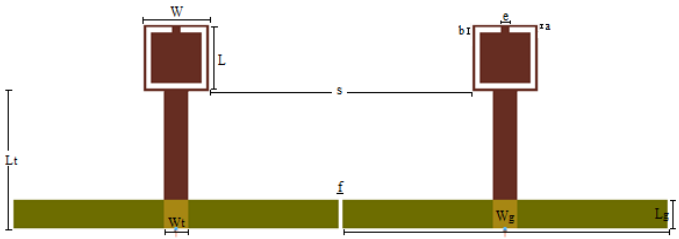

Figure 5 The configuration of two-element MIMO antenna with single external SRR.

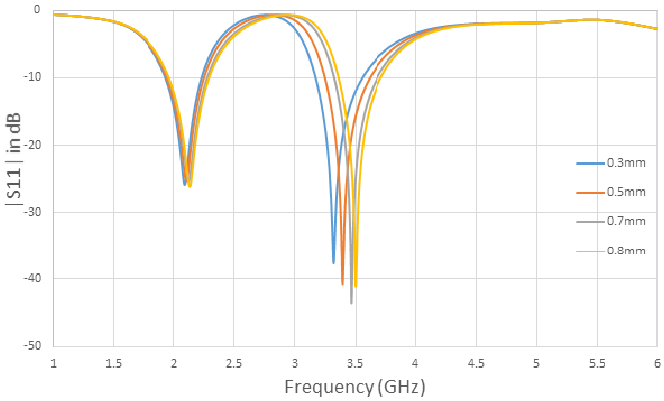

Figure 6 The reflection coefficient responses of the two-element MIMO antenna with single external SRR for different SRR widths (a).

After studying each parameters of the antenna to find the best antenna parameters and to get the requested triple band, two designs of the MIMO antenna will explained in the next two sections.

III. BEST IMPEDANCE BANDWIDTH ANTENNA DESIGN

Using two MIMO antennas with split ring resonators printed on the patch antenna and decrease the ground length to produce the triple bands, Table 4 shown the parameters of the best performance with the newly introduced parameters defined as depicted in Fig. 7.

The simulation results for the reflection coefficient and isolation characteristics are depicted in Fig. 8 also the corresponding E-plane cuts at the center frequencies of the operating bands of interest are depicted in Fig 9.

Table 4 The parameters values of the design MIMO antenna for the best the reflection coefficient

Parameter	Value (mm)	Parameter	Value (mm)
W	8.7	d	5.1
L	8.9	g	0.5
a	0.3	e	1
b	0.7	L_t	13.5
c	5.1	W_g	19.3
L_g	3.5	n	7.5
s	12.8	f	1.4

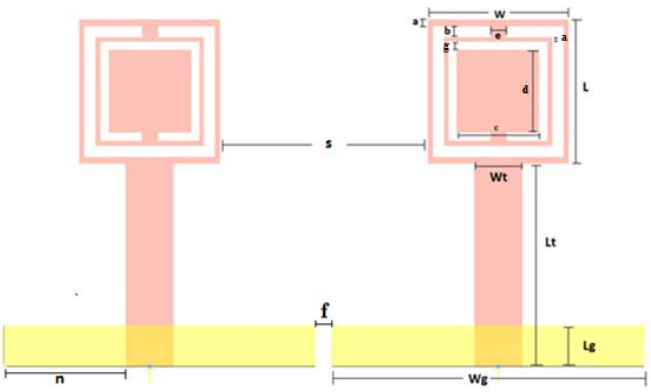

Figure 7 Two-element MIMO antenna configuration and parameter definition.

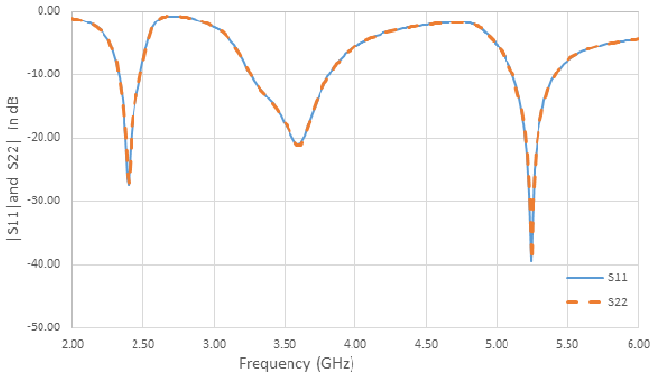

(a)

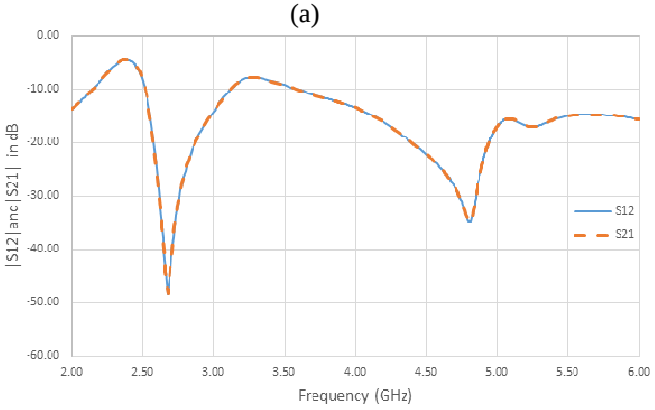

(b)

Figure 8 Reflection coefficient (a) and isolation (b) responses of the two-element MIMO antenna design of Fig.1 with the parameter setting of Table 2.

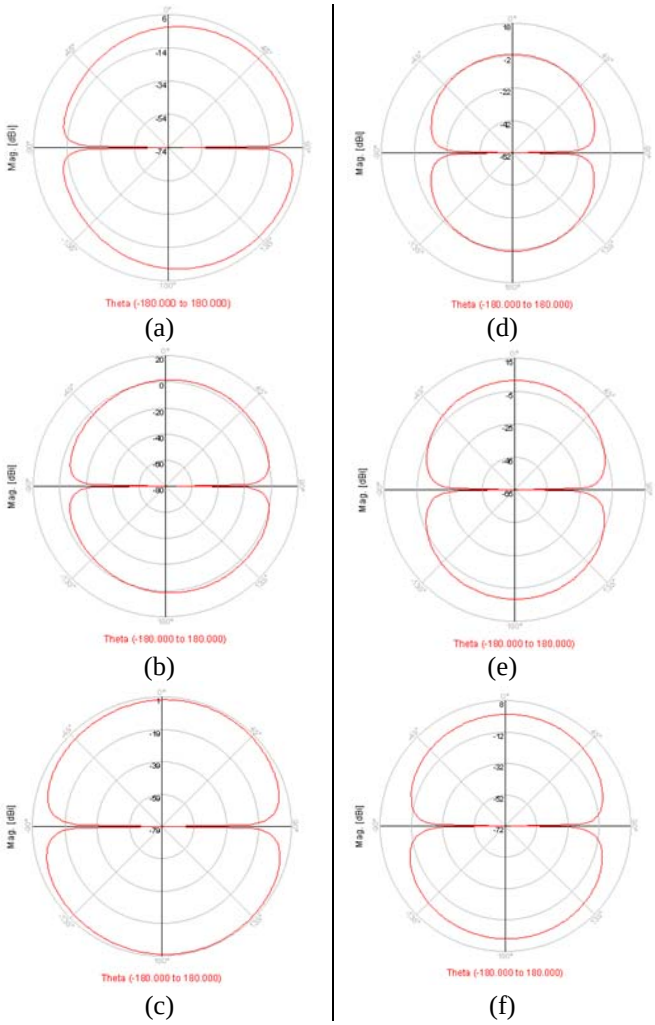

Figure 9 (a), (b) and (c) E-plane cuts when one of the elements is excited while the other is terminated in a matched load at 2.4, 3.55 and 5.25 GHz. (d), (e) and (f) 3Dradiation pattern when both elements are equally excited at 2.4, 3.55 and 5.25 GHz.

Table 5 summarizes the results obtained for the antenna gain (G), directivity (D), and efficiency for the three bands of interest and for both excitation scenarios.

Table 5 The gain, directivity, and efficiency of the three bands when only a single element is driven and when both elements are equivalently driven.

Band (GHz)	No. of Antennas	Gain (dB)	Directivity (dB)	Efficiency (%)
2.320 - 2.485	1	2.2	5.25	45
	2	2	3	75
3.250 - 3.825	1	2.73	4.25	70
	2	3.89	3.9	99
5.10 - 5.41	1	0.5	3.83	45
	2	2.95	4.78	60

IV. MIMO ANTENNA PERFORMANCE WITH A TWO-SIDED METAMATERIAL GRID AND NEUTRALIZING LINE.

The isolation between the two antenna elements could be improved using a neutralizing line as depicted in Fig.10 [20]. The NL works as a distributed inductance acting to neutralize the inherent capacitive coupling effect between the closely aligned patch radiators. This helps reducing the mutual impedance between the two antenna elements at their excitation ports helping thereby to increase the isolation between them.

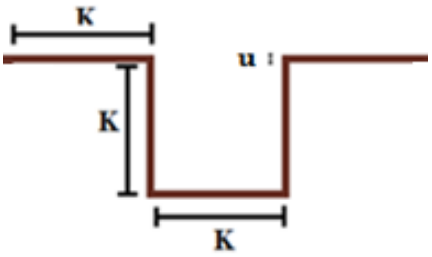

Figure 10 The configuration of two-element MIMO antenna with the (NL) where K=4.5mm and U=0.25 mm.

The printed metamaterial cell geometry and parameter definitions are depicted in Fig. 11, and the parameters are set as shown in Table 6 [21]. Finite two-dimensional grids of these printed cells will be incorporated on the front and back sides of the antenna as shown in fig. 12

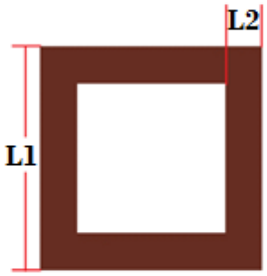

Figure 11 The geometry and parameters of metamaterial unit cell [21].

Table 6 The parameters description and values of metamaterial unit cell.

Parameter	Description	Value (mm)
L1	Length of the metamaterial cell	1.5
L2	Width of the metamaterial cell	0.25
L3	Distance between two cells	0.25
L4	Distance between metamaterial and TL	0.75

The simulation results for the reflection coefficient and isolation characteristics are depicted in fig.13 also the E-plane cuts at the center frequencies of the operating bands of interest are depicted in fig 14.

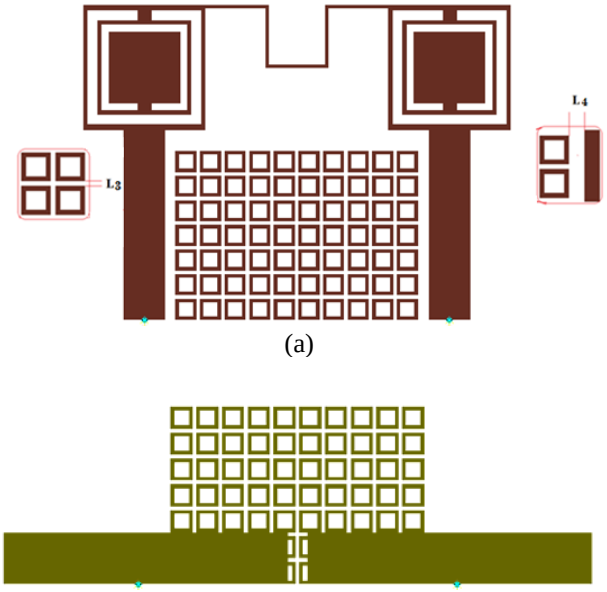

(a)

(b)

Figure 12 The configuration of two antenna MIMO with the (NL) and metamaterial use in both the front and ground layer (a) Front view, (b) Rear

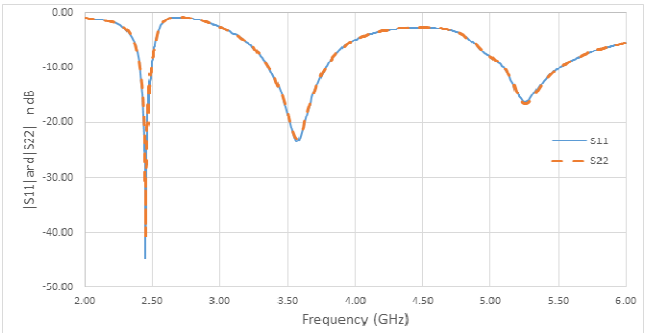

(a)

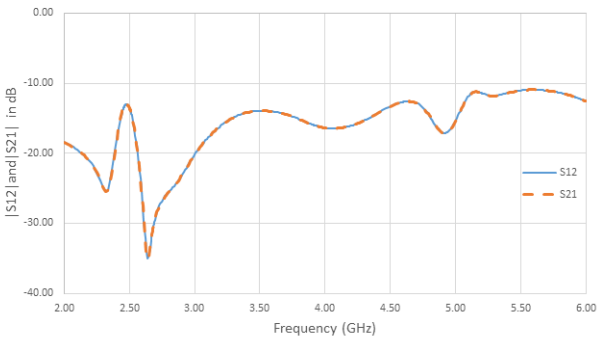

(b)

Figure 13 The reflection coefficient (a) and isolation (b) responses of the two-element MIMO antenna design of Fig. 17 with the parameter setting of Table 4, 4.2 K=4.5mm2 and U=0.25 mm2.

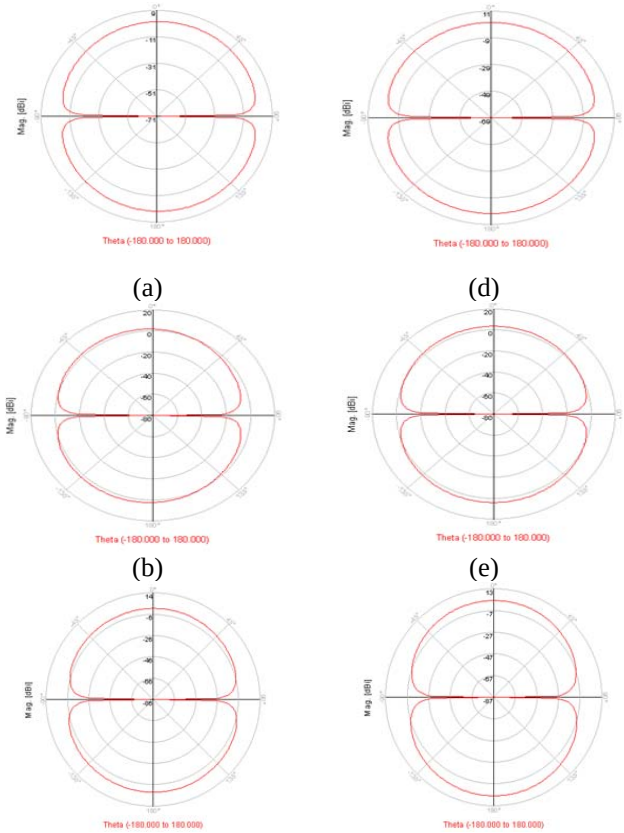

(a) (d)

(b) (e)

(c) (f)

Figure 14 (a), (b) and (c) E-plane cuts when one of the elements is excited while the other is terminated in a matched load at 2.45, 3.55 and 5.25 GHz. (d), (e) and (f) 3D radiation pattern when both elements are equally excited at 2.45, 3.55 and 5.25 GHz.

Table 7 summarizes the results obtained for the antenna gain (G), directivity (D), and efficiency for the three bands of interest and for both excitation scenarios.

Table 7 The bandwidth, Isolation, Gain, Directivity and efficiency of the three bands with NL and metamaterialin both layer of two cases.

Band (GHz)	Isolation (dB)	No: of Antenna	G (dB)	D (dB)	Efficiency (%)
2.40-2.49	13	1	0.9	3.19	60
		2	2.55	3	90
3.35-3.80	13.5	1	2.9	4.16	75
		2	3.9	4	99
5.09 - 5.55	12	1	2	4.25	60
		2	4.05	5.02	80

V. Practical Results

Two network measurements were performed using Agilent ENA Series network analyzer (model E5071C) for the two prototype in figs 15 and 16. The variation of the reflection coefficients (S11,S22) and the isolation (S21,S12) versus frequency were measured for the two designs. Table 8 present the bandwidth and isolation of the simulation and measurement results for the two prototypes both result clearly shows the three bands for the first design: (2.2-2.7) GHz, (3.5-4.5) GHz, and (5.8-6.8) GHz; and for the second design (2.35-2.7) GHz, (3.45-4.45) GHz, and (5.6-6.6) GHz. In addition, it can be noticed that the isolation is more than 16 dB in all of the bands for both prototypes. Figure 17 and 18 show the reflection coefficient and the isolation of the practical and simulation measurements for the first and second design.

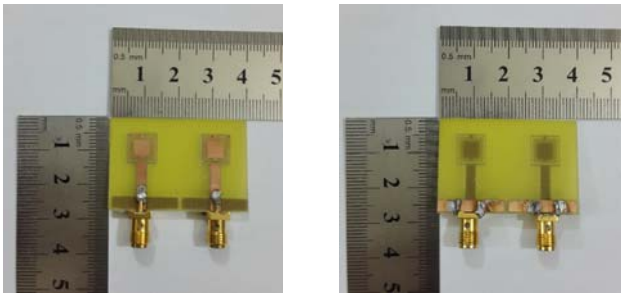

(a) (b)

Figure 15 A prototype of the best triple band performance MIMO antenna.
(a) Front view; (b) Rear view.

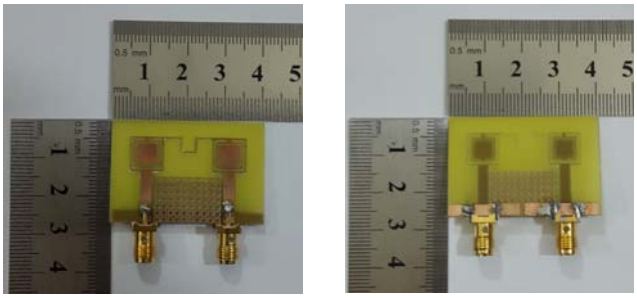

(a) (b)

Figure 16 A prototype of the NL and metamaterial-enhanced MIMO antenna. (a) Front view; (b) Rear view.

Table 8 The Bandwidth and Isolation of the Simulation and Measurement Results for the two Prototypes.

Prototype	Simulation Results		Measurement Results	
	Bandwidth	Isolation	Bandwidth	Isolation
First	2.320-2.485	5	2.25-2.65	16.5
	3.25-3.825	10	3.50-4.50	16.2
	5.10 - 5.41	15	5.80-6.80	18.5
Second	2.40-2.49	13	2.35-2.60	17
	3.35-3.80	13.5	3.45-4.45	22
	5.09-5.55	12	5.6-6.6	16.5

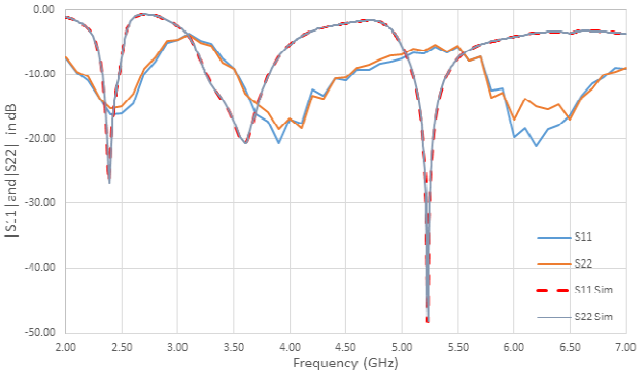

(a)

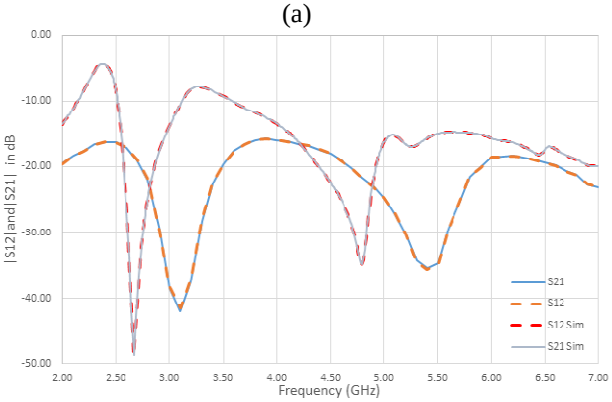

(b)

Figure 17 Simulated and measured reflection and isolation characteristics of the best triple band performance MIMO antenna design. (a) Reflection coefficient; (b) Isolation.

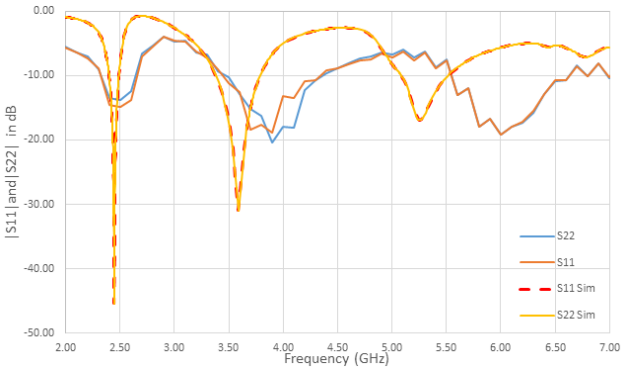

(a)

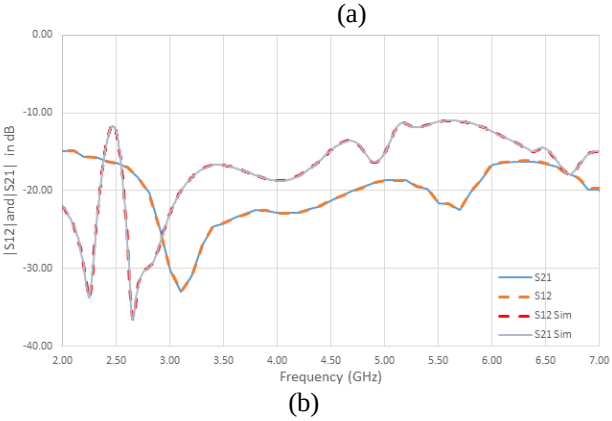

(b)

Figure 18 Simulated and measured reflection and isolation characteristics of the NL and metamaterial-enhanced MIMO antenna design. (a) Reflection coefficient; (b) Isolation.

VI. CONCLUSIONS

In this work, a metamaterial-enhanced two-element MIMO antenna which covers the following ranges of frequencies: (2.4-2.485) GHz, (5.1-5.35) GHz for Wi-Fi (IEEE 802.11) and (3.35-3.8) GHz for Wi-max (IEEE 802.16.2005) has been designed, simulated, and fabricated. The proposed design makes use of three main geometrical constructs to achieve the above goal. Firstly, it incorporates SRR construct along with a reduced-length ground plane to produce the triple band performance of interest. Secondly, it incorporates a neutralizing line construct to improve the isolation between the two antenna elements. Finally, it incorporates a double-sided metamaterial grid to bring even more improvement in terms of isolation and radiation efficiency. The inclusion of the aforementioned design constructs helped achieving antenna miniaturization while maintaining the desired performance characteristics. The final antenna design dimensions are only 40×27.2 mm2 compared to the initial single-band (WiFi) MIMO design with the dimensions of 130×80 mm2.For the proposed MIMO array antennas with metamaterial, the radiation patterns within the operating frequency bands are relatively acceptable compared with omnidirectional ones.

The proposed antenna performance has been verified using Advance Design System (ADS) software package version 2013 from Agilent Inc. and it has been fabricated and tested successfully. The measurements of the fabricated antenna are almost similar to the simulation results but they are not typically the same due to the limited ability of the fabrication facilities.

REFERENCES

[1]. Mohammad S. Sharawi, Ahmed B. Numan and Daniel N. Aloi, “Isolation Improvement in a Dual-Band Dual Element MIMO Antenna System Using Capacitively Loaded Loops”, Progress In Electromagnetics Research, Vol. 134, 247–266, and 2013.

[2]. Yogesh Kumar Choukiker, Satish K. Sharma, and Santanu K. Behera, “Hybrid Fractal Shape Planar Monopole Antenna Covering Multiband Wireless Communications with MIMO Implementation for Handheld Mobile Devices”, IEEE Transactions on Antennas and Propagation, Vol. 62, No. 3, March 2014.

[3]. Nguyen Khac Kiem, Huynh Nguyen Bao Phuong, Quang Ngoc Hieu, and Dao Ngoc Chien, “A Novel Metamaterial MIMO Antenna with High Isolation for WLAN Applications” , Hindawi Publishing Corporation International Journal of Antennas and Propagation Volume 2015.

[4]. Kamili J. Babu, Rabah W. Aldhaheri, Mohammed Y. Talha, and Ibrahim S. Alruhaili, “Design of a Compact Two Element MIMO Antenna System with Improved Isolation”, Progress In Electromagnetics Research Letters, Vol. 48, 27–32, 2014.

[5]. Lanchao Zhang, Tao Jiang, and Yingsong Li, “Design of a High Isolation Dual-band MIMO Antenna for WLAN and WIMAX Applications” , PIERS Proceedings, Prague, Czech Republic, July 6–9, 2015.

[6]. Jeet Ghosh, Sandip Ghosal, Debasis Mitra, and Sekhar Ranjan Bhadra Chaudhuri, “Mutual Coupling Reduction between Closely Placed Microstrip Patch Antenna Using Meander Line Resonator”, Progress In Electromagnetics Research Letters, Vol. 59, 115–122, 2016.

[7]. You-Bao Wang, Shun Xiao, Bo Zhang, and Ye Wei1, “Design of Compact Microstrip Antenna Array with Decoupling Network” , Progress In Electromagnetics Research Letters, Vol. 60, 59–65, 2016.

[8]. D. A. Ketzaki, D. K. Ntaikos, N. K. Bourgis and T. V. Yioultsis, “Metamaterial-enhanced MIMO Antennas” , 2nd pan-Hellenic Conference on electronics and Telecommunication 2012.

[9]. Hamideh Kondori, Mohammad Ali Mansouri-Birjandi and Saeed Tavakoli, “Reducing Mutual Coupling in Microstrip Array Antenna Using Metamaterial Spiral Resonator” IJCSI International Journal of Computer Science Issues, Vol. 9, Issue 3, No 1, May 2012

[10]. Belgacem Aouadi and Jamel Belhaj Tahar “Enhancement of Characteristics of Antenna Arrays Employing S-Shaped Resonators” Journal of Electromagnetic Analysis and Applications, 2012, 4, 326-332.

[11]. Jiang Zhu and George V. Eleftheriades, “A Simple Approach for Reducing Mutual Coupling in Two Closely Spaced Metamaterial-Inspired Monopole Antennas” , IEEE Antennas and Wireless Propagation Letters, Vol. 9, 2010.

[12]. Youngki Lee, Deukhyeon Ga, and Jaehoon Choi, “Design of a MIMO Antenna with Improved Isolation Using MNG Metamaterial” , Hindawi Publishing Corporation International Journal of Antennas and Propagation Volume 2012.

[13]. IEEE 802.11 a/b/g/n Wi-Fi Standards and Facts AIR 802.

[14]. Deploying License-Exempt WiMAX Solutions intel white paper

[15]. Jie-Huang Huang, Wen-Jiun Chang, and Christina F. Jou“Dual-Band MIMO Antenna with High Isolation Application by Using Neutralizing Line”Vol. 48, 15–19, 2014.

[16]. P. W. Kolb, T. S. Salter, J. A. McGee,H. D. Drew, and W. J. Padilla“Extreme subwavelength electric GHz metamaterials”JOURNAL OF APPLIED PHYSICS 110, 054906 (2011).